

# Plumbagin induces G<sub>2</sub>-M arrest and autophagy by inhibiting the AKT/mammalian target of rapamycin pathway in breast cancer cells

Po-Lin Kuo,<sup>1</sup> Ya-Ling Hsu,<sup>2</sup> and Chien-Yu Cho<sup>3</sup>

<sup>1</sup>Cell Biology Laboratory, Department of Biotechnology and <sup>2</sup>Department of Pharmacy, Chia-Nan University of Pharmacy and Science, Tainan, Taiwan; and <sup>3</sup>Graduate Institute of Natural Products, Kaohsiung Medical University, Kaohsiung, Taiwan

## Abstract

This study is the first to investigate the anticancer effect of plumbagin in human breast cancer cells. Plumbagin exhibited cell proliferation inhibition by inducing cells to undergo G<sub>2</sub>-M arrest and autophagic cell death. Blockade of the cell cycle was associated with increased p21/WAF1 expression and Chk2 activation, and reduced amounts of cyclin B1, cyclin A, Cdc2, and Cdc25C. Plumbagin also reduced Cdc2 function by increasing the association of p21/WAF1/Cdc2 complex and the levels of inactivated phospho-Cdc2 and phospho-Cdc25C by Chk2 activation. Plumbagin triggered autophagic cell death but not predominantly apoptosis. Pretreatment of cells with autophagy inhibitor bafilomycin suppressed plumbagin-mediated cell death. We also found that plumbagin inhibited survival signaling through the phosphatidylinositol 3-kinase/AKT signaling pathway by blocking the activation of AKT and downstream targets, including the mammalian target of rapamycin, forkhead transcription factors, and glycogen synthase kinase 3 $\beta$ . Phosphorylation of both of mammalian target of rapamycin downstream targets, p70 ribosomal protein S6 kinase and 4E-BP1, was also diminished. Overexpression of AKT by AKT cDNA transfection decreased plumbagin-mediated autophagic cell death, whereas reduction of AKT expression by small interfering RNA potentiated the effect of plumbagin, supporting the inhibition of AKT being beneficial to autophagy. Furthermore, suppression of AKT by plumbagin enhanced the activation of Chk2, resulting in increased inactive phosphorylation of Cdc25C and Cdc2. Further investigation revealed that plumbagin inhibition of cell growth was also

evident in a nude mouse model. Taken together, these results imply a critical role for AKT inhibition in plumbagin-induced G<sub>2</sub>-M arrest and autophagy of human breast cancer cells. [Mol Cancer Ther 2006;5(12):3209–21]

## Introduction

Autophagic cell death is an important physiologic process occurring in all eukaryotic cells (1, 2). The characterization of autophagic cell death is revealed by massive degradation of cellular contents, including portions of the cytoplasm and intracellular organelles, by means of complicated intracellular membrane/vesicle reorganization and lysosomal hydrolases (1–3). Autophagic cell death is involved in development and stress responses and has been observed in several human diseases such as neurodegenerative disease, muscular disorders, and pathogen resistance (2). Furthermore, like apoptosis, autophagic cell death is found to be suppressed in malignant tumors and involved in tumorigenesis. A number of studies have reported that autophagy is activated in response to  $\gamma$ -irradiation and various anticancer therapies (2, 4, 5). Several molecular and cell signaling pathways have been implicated in regulating autophagy, such as BECN1, death-associated protein kinase, death-associated related protein kinase 1, mitogen-activated kinase, and phosphatidylinositol 3-kinase (PI3K)/AKT/mammalian target of rapamycin (mTOR) pathways (1, 2, 6). However, detailed mechanisms of the autophagic cell signaling pathway are poorly understood.

PI3K/AKT signaling has been found to be involved in the survival and proliferation of a variety of tumor cells, including breast cancers (7, 8). Hyperactivation of PI3K/AKT has resulted in altering the response of tumor cells to chemotherapy and irradiation (9, 10). PI3K is a heterodimer of the regulatory p85 and catalytic p110 subunits. A variety of growth factors can activate PI3K through activation of their cognate receptors, leading to the activation of AKT signaling. AKT mediates a variety of biological functions, including glucose uptake, protein synthesis, and inhibition of cell death (8). AKT can mediate cell survival and growth by regulating both posttranslational mechanisms and gene transcription. AKT activity is regulated by phosphorylation on two regulatory residues, Thr<sup>308</sup> in the activation loop of the catalytic domain and Ser<sup>473</sup> in the regulatory domain (8). Once activated, AKT can promote cell survival by inhibiting type I (apoptosis) and type II (autophagy) cell death by phosphorylation of several signaling proteins, including cyclic AMP response element-binding protein, mTOR proteins, forkhead transcription factors (FKHR), and glycogen synthase kinase-3 (GSK-3; refs. 1, 2, 8, 11). mTOR is a serine-threonine kinase that regulates the function of transcriptional regulators p70 ribosomal protein S6 kinase

Received 8/9/06; revised 9/20/06; accepted 10/20/06.

**Grant support:** National Science Council of Taiwan grant NSC 94-2320-B-041-007.

The costs of publication of this article were defrayed in part by the payment of page charges. This article must therefore be hereby marked advertisement in accordance with 18 U.S.C. Section 1734 solely to indicate this fact.

**Requests for reprints:** Po-Lin Kuo, Cell Biology Laboratory, Department of Biotechnology, Chia-Nan University of Pharmacy and Science, Tainan 717, Taiwan. Phone: 886-6-266-4911, ext. 520; Fax: 886-6-266-2135. E-mail: kuopolin@seed.net.tw

Copyright © 2006 American Association for Cancer Research.

doi:10.1158/1535-7163.MCT-06-0478

(p70S6 kinase) and 4E-BP1 (8, 12). Recent studies have shown that the inhibition of AKT and its downstream target mTOR contributes to the initiation of autophagy (11, 13). Therefore, mTOR signaling has emerged as an important and attractive therapeutic target for cancer therapy.

Eukaryotic cell cycle progression involves the sequential activation of cyclin-dependent kinases, the activation of which is dependent on their association with cyclins (14). The complex formed by the association of Cdc2 and cyclin B1 plays a major role in the entry into mitosis (14). Regulation of Cdc2 activity is controlled at three levels. First, Cdc2 is inactive as a monomer and must bind with cyclin B during the G<sub>2</sub>-M transition (14, 15). Second, it is also regulated by cyclin-dependent kinase inhibitors, such as p21/WAF1 and p27/KIP, binds to cyclin/cyclin-dependent kinase complexes, and prevents kinase activation (14). Finally, a series of reversible phosphorylations regulates the activity of the Cdc2/cyclin B complex. Phosphorylation of Cdc2 on Thr<sup>161</sup> by cyclin-dependent kinase-activating kinase is essential for Cdc2 kinase activity (14). In contrast, Cdc2 is committed to inhibitory phosphorylation at Tyr<sup>15</sup> and Thr<sup>14</sup> by Wee1/Mik1/Myt1 kinases (14, 16). During the G<sub>2</sub>-M transition, Cdc2 is rapidly converted into the active form by Tyr<sup>15</sup> dephosphorylation catalyzed by the Cdc25 phosphatase. In mammalian cells, Chk2 phosphorylated Cdc25C at Ser<sup>216</sup>, a site known to be involved in negative regulation of Cdc25C (17). Phosphorylation of Cdc25C on Ser<sup>216</sup> interferes with the ability of Cdc25C to promote mitotic entry (17). Thus, the activity of Chk2 exceeds that of Cdc25C in the G<sub>2</sub>-M phase, and this regulation is therefore crucial to the G<sub>2</sub>-M transition.

Plumbagin (5-hydroxy-2-methyl-1,4-naphthoquinone), a quinonoid constituent isolated from the root of *Plumbago zeylanica* L. (also known as "Chitrak"), has been shown to exert anticarcinogenic, antiatherosclerotic, and antimicrobial effects (18–21). The root of *P. zeylanica* L. has been used in Indian medicine for ~2,750 years and its component possess antiatherogenic, cardiogenic, hepatoprotective, and neuroprotective properties (19). In short, plumbagin has exhibited anticancer and antiproliferation properties in a variety of cell lines and animal models (22, 23). In this study, we determined the cell growth inhibition activity of plumbagin by using *in vitro* and *in vivo* experimental models and examined its effect on cell cycle distribution and autophagic cell death in two human breast cancer cell lines, MDA-MB-231 and MCF-7. Furthermore, to establish the anticancer mechanism of plumbagin, we assayed the levels of cell cycle control- and autophagy-related molecules, which are strongly associated with the cell death signal transduction pathway and affect the chemosensitivity of tumor cells to anticancer agents.

## Materials and Methods

### Materials

FCS, RPMI 1640, penicillin G, streptomycin, and amphotericin B were obtained from GIBCO-BRL Life Technologies, Inc. (Gaithersburg, MD). Plumbagin, acridine orange, mono-

dansylcadaverine, bafilomycin, DMSO, RNase, trypsin-EDTA, and propidium iodide were purchased from Sigma Chemical (St. Louis, MO). 2,3-Bis[2-methoxy-4-nitro-5-sulphophenyl]-2H-tetrazolium-5-carboxanilide inner salt (XTT) was obtained from Roche Diagnostics GmbH (Mannheim, Germany). PI3K p85, PI3K p110 $\alpha$ , PI3K p110 $\gamma$ , mTOR, phospho-mTOR, p70S6K, and phospho-p70S6K antibodies and AKT activity assay kit were obtained from Cell Signaling Technology (Beverly, MA). ATK cDNA plasmid was obtained from Upstate Biotechnology, Inc. (Lake Placid, NY). AKT1 small interfering RNA (siRNA) and control siRNA were purchased from Ambion (Austin, TX). Beclin-1 siRNA was purchased from Dharmacon (Boulder, CO).

### Cell Culture

MCF-7 (ATCC HTB-22) and MDA-MD-231 cells (ATCC HTB-26) were obtained from the American Type Cell Culture Collection (Manassas, VA). MCF-7 cells were cultured in DMEM with nonessential amino acids, 0.1 mmol/L sodium pyruvate, 10  $\mu$ g/mL insulin, and 10% FCS. MDA-MB-231 cells were cultured in RPMI 1640 (Life Technologies, Inc., Grand Island, NY) supplemented with 10% FCS and 1% penicillin-streptomycin solution (Life Technologies).

### Cell Proliferation and Clonogenic Assay

Inhibition of cell proliferation by plumbagin was measured by XTT assay. Cells were plated in 96-well culture plates (1  $\times$  10<sup>4</sup> per well). After 24-h incubation, the cells were treated with plumbagin (0, 2.5, 5, 10, and 20  $\mu$ mol/L) for 48 h. Fifty microliters of XTT test solution, which was prepared by mixing 5 mL of XTT-labeling reagent with 100  $\mu$ L of electron coupling reagent, were then added to each well. The absorbance was measured on an ELISA reader (Multiskan EX, Labsystems, Helsinki, Finland) at a test wavelength of 492 nm and a reference wavelength of 690 nm. Data were calculated as the percentage of inhibition by the following formula: % inhibition = [100 – (A<sub>t</sub> / A<sub>s</sub>)  $\times$  100]  $\times$  %. A<sub>t</sub> and A<sub>s</sub> indicated the absorbances of the test substances and solvent control, respectively.

To determine long-term effects, cells were treated with plumbagin at various concentrations for 1 h. After being rinsed with fresh medium, cells were allowed to grow for 14 days to form colonies, which were then stained with crystal violet (0.4 g/L; Sigma). Clonogenic assay was used to elucidate the possible differences in long-term effects of plumbagin on human breast cells.

### Cell Cycle Analysis

To determine cell cycle distribution analysis, 5  $\times$  10<sup>5</sup> cells were plated in 60-mm dishes and treated with plumbagin (0, 4, and 8  $\mu$ mol/L) for 6 h. After treatment, the cells were collected by trypsinization, fixed in 70% ethanol, washed in PBS, resuspended in 1 mL of PBS containing 1 mg/mL RNase and 50  $\mu$ g/mL propidium iodide, incubated in the dark for 30 min at room temperature, and analyzed using EPICS flow cytometer (Beckman-Coulter, Inc., Miami, FL). The data were analyzed using Multicycle software (Phoenix Flow Systems, San Diego, CA).

### Apoptosis Assay

Cells (1  $\times$  10<sup>6</sup>) were treated with vehicle alone (0.1% DMSO) and various concentrations of plumbagin and

cisplatin for 48 h, then collected by centrifugation. Pellets were lysed in DNA lysis buffer [10 mmol/L Tris (pH 7.5), 400 mmol/L EDTA, and 1% Triton X-100] and then centrifuged. The supernatant obtained was incubated overnight with proteinase K (0.1 mg/mL) and then with RNase (0.2 mg/mL) for 2 h at 37°C. After extraction with phenol/chloroform (1:1), the DNA was separated in 2% agarose gel and visualized by UV after staining with ethidium bromide. Quantitative assessment of apoptotic cells was assessed by the terminal deoxynucleotidyl transferase-mediated dUTP nick end labeling (TUNEL) method, which examines DNA strand breaks during apoptosis using the BD ApoAlert DNA Fragmentation Assay Kit.

#### Detection and Quantification of Acidic Vesicular Organelles with Acridine Orange Staining

Autophagy is the process of sequestering cytoplasmic proteins into lytic components and is characterized by the formation and promotion of acidic vesicular organelles. To assess the occurrence of acidic vesicular organelles, we treated tumor cells with plumbagin for the indicated times and then stained them with acridine orange. Briefly, cells were incubated with acridine orange (1 µg/mL) for 15 min, then examined under a fluorescent microscope (5, 11, 24). To quantify the development of acidic vesicular organelles, plumbagin-treated cells were stained with acridine orange (1 µg/mL) for 15 min and removed from the plate with trypsin-EDTA. The stained cells were then analyzed using EPICS flow cytometer (11).

#### Detection of Autophagic Vacuoles with Monodansylcadaverine

Autophagic vacuoles were also detected with monodansylcadaverine by incubating cells with monodansylcadaverine (50 µmol/L) in PBS at 37°C for 10 min. After incubation, cells were washed four times with PBS and immediately analyzed by fluorescent microscopy using an inverted microscope (Nikon Eclipse TE 300, Dusseldorf, Germany) equipped with a filter system (excitation wavelength, 380 nm; emission filter, 525 nm; ref. 25).

#### Electron Microscopy

Cells or tumor sections were directly fixed with 1% glutaraldehyde and postfixed with 2% osmium tetroxide. The cell pellets or sections were embedded in epon resin. Representative areas were chosen for ultrathin sectioning and viewed with a JEM 1010 transmission electron microscope (JEOL, Peabody, MA).

#### Immunoprecipitation/Immunoblot and AKT Kinase Activity Assays

Cells were treated with various concentrations of plumbagin for the indicated times. For immunoblotting, the cells were lysed on ice for 40 min in a solution containing 50 mmol/L Tris, 1% Triton X-100, 0.1% DS, 150 mmol/L NaCl, 2 mmol/L Na<sub>3</sub>VO<sub>4</sub>, 2 mmol/L EGTA, 12 mmol/L β-glycerolphosphate, 10 mmol/L NaF, 16 µg/mL benzamidine hydrochloride, 10 µg/mL phenanthroline, 10 µg/mL aprotinin, 10 µg/mL leupeptin, 10 µg/mL pepstatin, and 1 mmol/L phenylmethylsulfonyl fluoride. The cell lysate was centrifuged at 14,000 × g for 15 min and the supernatant fraction collected for immuno-

blotting. Equivalent amounts of protein were resolved by SDS-PAGE (10–12%) and transferred to polyvinylidene difluoride membranes. After blocking for 1 h in 5% nonfat dry milk in TBS, the membrane was incubated with the desired primary antibody for 1 to 16 h. The membrane was then treated with appropriate peroxidase-conjugated secondary antibody and the immunoreactive proteins were detected using an enhanced chemiluminescence kit (Amersham Biosciences Inc., Piscataway, NJ) according to the manufacturer's instructions. AKT activity was determined using kits from Cell Signaling Technology according to the manufacturer's instructions.

#### Transient Transfection of Activated AKT-tag cDNA

Transfection of MDA-MB-231 cells was carried out using Lipofectamine 2000 reagent. MDA-MB-231 cells were exposed to the mixture of Lipofectamine 2000 reagent and AKT cDNA plasmid or empty vector with pM1-β-Gal expression vector (Roche) for 6 h. Then, 8 mL of RPMI 1640 with 20% fetal bovine serum were added to each culture dish. After 18 h of incubation, fresh RPMI 1640 was added and the cells were incubated for another 2 days. Transfection efficiencies were determined by measuring β-galactosidase activity using the β-galactosidase ELISA kit (Roche).

#### SiRNA Knockdown of AKT and Beclin-1 Expression

Breast cancer cell monolayers were transfected with Beclin-1, AKT1 siRNA duplexes (sense, GGGCACUUUCG-GCAAGGUGtt; antisense, CACCUUGCCGAAAGUG-CCCtt), or nonspecific control siRNA duplexes (Upstate Biotechnology) by using Lipofectamine 2000 (Invitrogen, Carlsbad, CA). Immunoblot analyses showed that Beclin-1 expression was aborted, AKT remained low but detectable, and expression of β-actin was unaffected by siRNA treatment.

#### In vivo Tumor Xenograft Study

Female nude mice [6 weeks old; BALB/cA-nu (*nu/nu*)] were purchased from the National Science Council Animal Center (Taipei, Taiwan) and maintained in pathogen-free conditions. MDA-MB-231 cells were injected s.c. into the flanks of the mice (5 × 10<sup>6</sup> in 200 µL) and tumors were allowed to develop for ~30 days until they reached 50 mm<sup>3</sup>, then treatment was initiated. Twenty mice were randomly divided into two groups. The mice in the plumbagin-treated group were i.p. injected daily with plumbagin in a clear solution containing 25% polyethylene glycol (2 mg/kg of body weight) in a volume of 0.2 mL. The control group was treated with an equal volume of vehicle. After transplantation, tumor size was measured using calipers and tumor volume was estimated according to the following formula: tumor volume (mm<sup>3</sup>) =  $L \times W^2 / 2$ , where *L* is the length and *W* is the width. Tumor-bearing mice were sacrificed after 60 days. Xenograft tumors, as well as other vital organs of the treated and control mice, were harvested and fixed in 4% formalin, embedded in paraffin, and cut into 4-µm sections for histologic study.

#### Statistical Analysis

Data were expressed as means ± SD. Statistical comparisons of the results were made using ANOVA. Significant differences (*P* < 0.05) between the means of control and plumbagin-treated cells were analyzed by Dunnett's test.

## Results

### Plumbagin Inhibits Cell Proliferation and Clonogenic Survival in MDA-MB-231 and MCF-7 Cells

To investigate the potential cell growth inhibition of plumbagin in breast cancer, we first examined the effect of plumbagin on cell proliferation and clonogenic survival in MDA-MB-231 and MCF-7 cells. As shown in Fig. 1A, plumbagin inhibited cell growth in both cancer cell lines in a concentration-dependent manner. The  $IC_{50}$  values of plumbagin were 4.4  $\mu\text{mol/L}$  for MDA-MB-231 and 3.2  $\mu\text{mol/L}$  for MCF-7.

Additional experiments were done to determine the antitumor activities of plumbagin inhibition when analyzed by *in vitro* clonogenic assays. *In vitro* clonogenic assays correlated very well with *in vivo* assays of tumorigenicity in nude mice (26, 27). Figure 1B and C shows the effects of plumbagin on the relative clonogenicity of the control and plumbagin-treated MDA-MB-231 and MCF-7 cells. Clonogenicity of both cancer lines was reduced in a concentration-dependent manner after exposure to plumbagin.

### Plumbagin Induces Cell Cycle Arrest and Regulates the Expression of Cell Cycle-Related Proteins in MDA-MB-231 and MCF-7 Cells

To examine the mechanism responsible for plumbagin-mediated cell growth inhibition, cell cycle distribution was

evaluated using flow cytometric analysis. The results showed that treating cells with plumbagin caused a significant inhibition of cell cycle progression in both cancer cell lines at 6 h (Fig. 2A), resulting in a clear increase in the percentage of cells in the  $G_2$ -M phase when compared with the control.

Next, we assessed the effects of plumbagin on cell cycle-related regulating factor. Plumbagin treatment of the cells resulted in a time-dependent decrease in the protein expression of cyclin A, cyclin B1, Cdc2, and Cdc25C in both cancer cell lines (Fig. 2B). In addition, exposure of cells to plumbagin for 3 h resulted in an increase in levels of inactive phospho-Cdc2 (Tyr<sup>15</sup>) and phospho-Cdc25C (Ser<sup>216</sup>). Exposure of breast cancer cells to 8  $\mu\text{mol/L}$  plumbagin resulted in rapid and sustained activation of Chk2 (phosphorylation at Ser<sup>345</sup>). Results from time-dependent studies have indicated that increasing functional Chk2 by increasing phosphorylation was followed by an increase in phospho-Cdc25C, which in turn increased phospho-Cdc2 (Fig. 2B). We suggest that Cdc2 and Cdc25C functions were inhibited by an increase in Chk2 function. Furthermore, the association of p21/WAF1 and Cdc2 increased in a time-dependent manner in plumbagin-treated breast cancer cell lines, as determined by immunoprecipitation assay (Fig. 2C).

### Plumbagin Does Not Predominantly Induce Apoptosis in MDA-MB-231 and MCF-7 Cells

Our previous published study showed that plumbagin induces apoptosis in human lung cancer A549 cells (28). At that time, we investigated whether plumbagin could also induce apoptosis in breast cancer. The TUNEL results showed that concentrations of 4 and 8  $\mu\text{mol/L}$  plumbagin induced only a small amount of apoptotic cell death in MDA-MB-231 and MCF-7 cells after 24 and 48 h of treatment (Fig. 3A), whereas treatment of cells with cisplatin (15  $\mu\text{g/mL}$ ) for 48 h resulted in a large increase in the amount of DNA breaks in both cell lines. When compared with cisplatin-treated cells, plumbagin treatment also failed to form the "DNA ladder" fragmentation, a typical marker of apoptosis, detectable by agarose gel electrophoresis at 48 h in MDA-MB-231 and MCF-7 at 4  $\mu\text{mol/L}$  (Fig. 3B).

To verify the possibility of apoptosis in plumbagin-treated breast cancer cells, we used pan-caspase inhibitor to block caspase activity in both cell lines and determined whether the cell proliferation inhibition was changed after plumbagin treatment. Blocking caspase activation resulted in a slight decrease in plumbagin-mediated proliferation inhibition in both cell lines, suggesting that plumbagin may induce a small number of breast cancer cells to undergo apoptosis (Fig. 3C).

### Plumbagin Induces Autophagy in MDA-MB-231 and MCF-7 Cells

Growing evidence indicates that nonapoptotic programmed cell death is principally attributed to autophagy (type II programmed cell death; ref. 2). The majority of plumbagin-treated breast cancer cells do not primarily display features typical of apoptosis. We next assessed

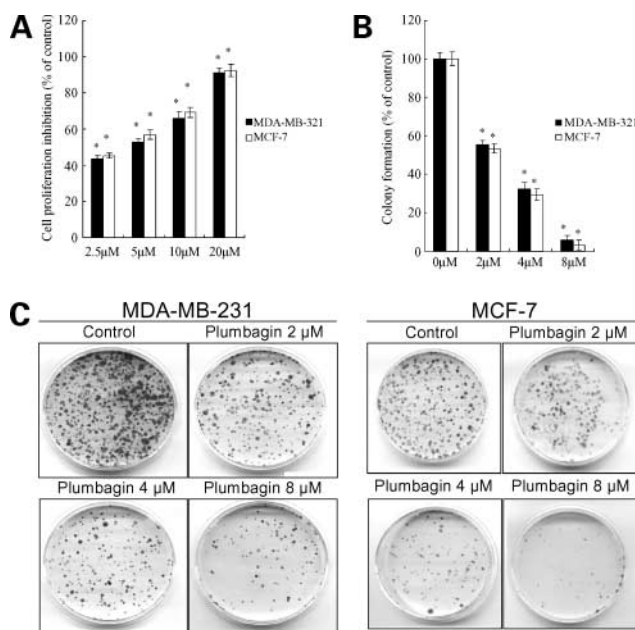
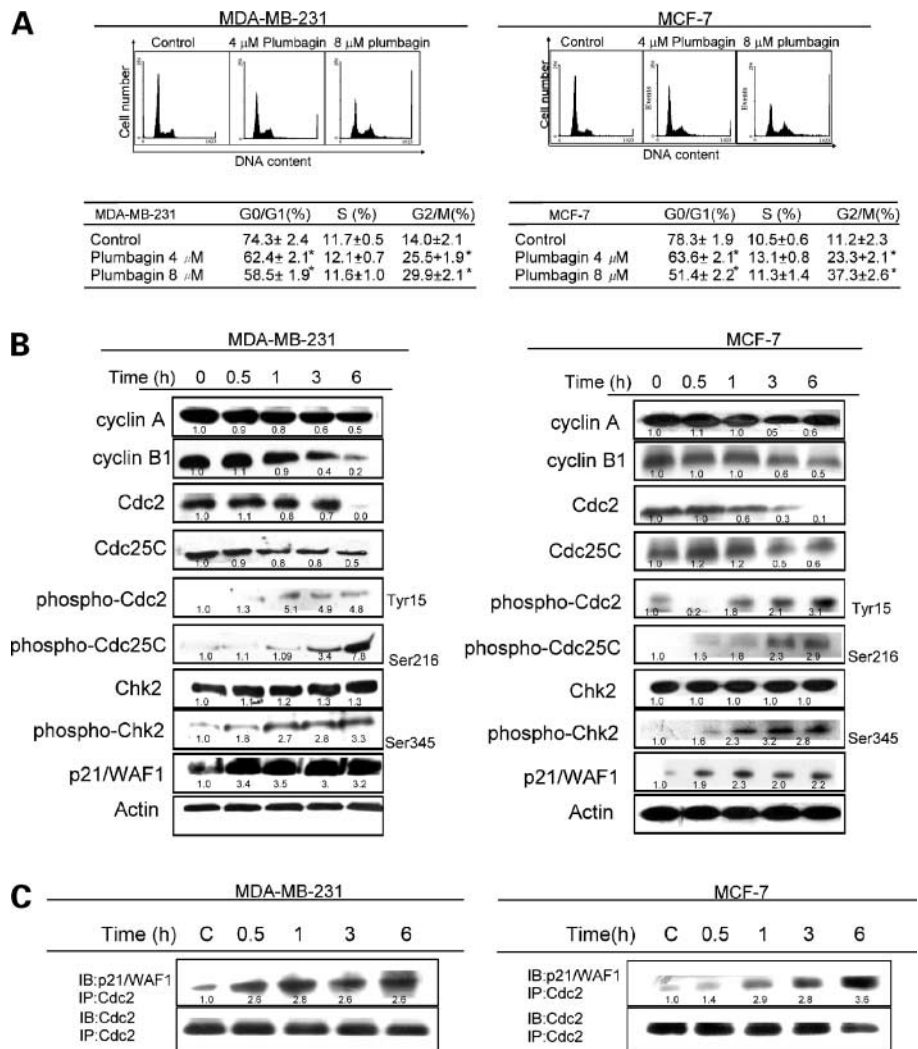


**Figure 1.** The inhibitory effects of plumbagin on cell proliferation and colony formation in MDA-MB-231 and MCF-7. **A**, inhibitory effect of plumbagin on cell proliferation in MDA-MB-231 and MCF-7. **B**, influence of breast cancer cells on the number of colony-forming cells, as evaluated by clonogenic assay. **C**, representative dishes by colony-forming assay. For (A), cell growth inhibition activity of plumbagin was assessed by XTT. For colony-forming assay, the clonogenic assay was done as described in Materials and Methods. Columns, mean of three determinations; bars, SD. Results shown are representative of three independent experiments. \*,  $P < 0.05$ , control versus plumbagin-treated cells.

**Figure 2.** Plumbagin induces cell cycle arrest and regulates the expression of cell cycle-related proteins in MDA-MB-231 and MCF-7 cells. **A**, distribution of cell cycles in plumbagin-treated cells. **B**, effect of plumbagin in cell cycle-related proteins. **C**, effect of plumbagin on association of p21/WAF1 and Cdc2. For **(A)**, cells were treated with vehicle and plumbagin for 6 h and cell cycle distribution was assessed by flow cytometry. For **(B)**, the cell cycle-related expression levels of 8  $\mu\text{mol/L}$  plumbagin-treated cancer cells were determined by Western blotting. For **(C)**, cell lysates were subjected to immunoprecipitation with anti-Cdc2, followed by immunoblotting analysis with anti-p21/WAF1. Representative of three independent experiments. \*,  $P < 0.05$ , control versus plumbagin-treated cells.



whether plumbagin induces autophagy in breast cancer. As shown in Fig. 4A, plumbagin treatment resulted in the appearance of acidic vesicular organelles when cells were stained with acridine orange after 24-h treatment. In addition, bafilomycin, an autophagy inhibitor (29), decreased the accumulation of red fluorescence in both control and plumbagin-treated cells. Because monodansylcadaverine accumulates in mature autophagic vacuoles, such as autophagolysosomes, but not in the early endosome compartment, monodansylcadaverine staining can be used to detect autophagic vacuoles. As shown in Fig. 4A, treatment of cells with plumbagin increased accumulation of monodansylcadaverine in comparison with the control. These results corroborate the observation that plumbagin treatment induces autophagic cell death in both cancer cell lines.

We also tested whether autophagy occurs in plumbagin-treated cells by using transmission electron microscopy. The results of transmission electron microscopy showed that in most of the cells, the nuclei maintained their integrity and displayed dispersed chromatin, which is not consistent with an apoptotic character. Normal

MDA-MB-231 cells had numerous membrane-bound vesicles, often containing organelles and other cellular fragments (Fig. 4B). In contrast, exposure of cells to 4 and 8  $\mu\text{mol/L}$  plumbagin resulted in the appearance of autophagocytic vacuoles after 12 and 24 h of treatment. Autophagocytic vacuoles contained extensively degraded organelles (Fig. 4B). The features of autophagy also manifested in MCF-7 after 24-h plumbagin treatment (Fig. 4B).

To quantify the accumulation of the acidic component, we did fluorescence-activated cell sorting analysis of acridine orange-stained cells using the FL3 channel to evaluate the bright red fluorescence and the FL1 channel to evaluate the green fluorescence (13). As shown in Fig. 4C, plumbagin (8  $\mu\text{mol/L}$ ) treatment increased the strength of red fluorescence from 3.1% to 19.9% and from 1.2% to 18.4% in MDA-MB-231 and MCF-7, respectively. In addition, bafilomycin decreased the strength of red fluorescence from 19.9% to 5.4% and from 18.4% to 3.3% in 8  $\mu\text{mol/L}$  plumbagin-treated MDA-MB-231 and MCF-7 cells.

To determine whether the autophagy seen in plumbagin-treated breast cancer cells is involved in cell death, we used siRNA to knock down Beclin-1 in MDA-MB-231 cells and determine whether autophagy is required for plumbagin-mediated cell proliferation inhibition. Reduction of Beclin-1 (Fig. 4D) resulted in a resistance to plumbagin-mediated proliferation inhibition in MDA-MB-231 cells (Fig. 4E).

#### Plumbagin Inhibits the Expression and Activity of PI3K/AKT/mTOR Pathway

We investigated whether PI3K/AKT/mTOR, which is important in regulating cell proliferation and autophagy,

is involved in plumbagin-mediated cell death in both cancer cell lines. Plumbagin treatment of cells was found to cause a significant reduction in the expression of the regulatory subunit of PI3K (p85) protein (Fig. 5A). Similarly, plumbagin caused a significant time-dependent decrease in the phosphorylation (Ser<sup>473</sup> and Thr<sup>308</sup>) of AKT protein in cells. Plumbagin treatment did not cause any change in the protein levels of total AKT, however. Exposure of breast cancer cells to plumbagin resulted in diminished levels of the phosphorylated (activated) form of mTOR (Ser<sup>2448</sup> and Ser<sup>2481</sup>), a

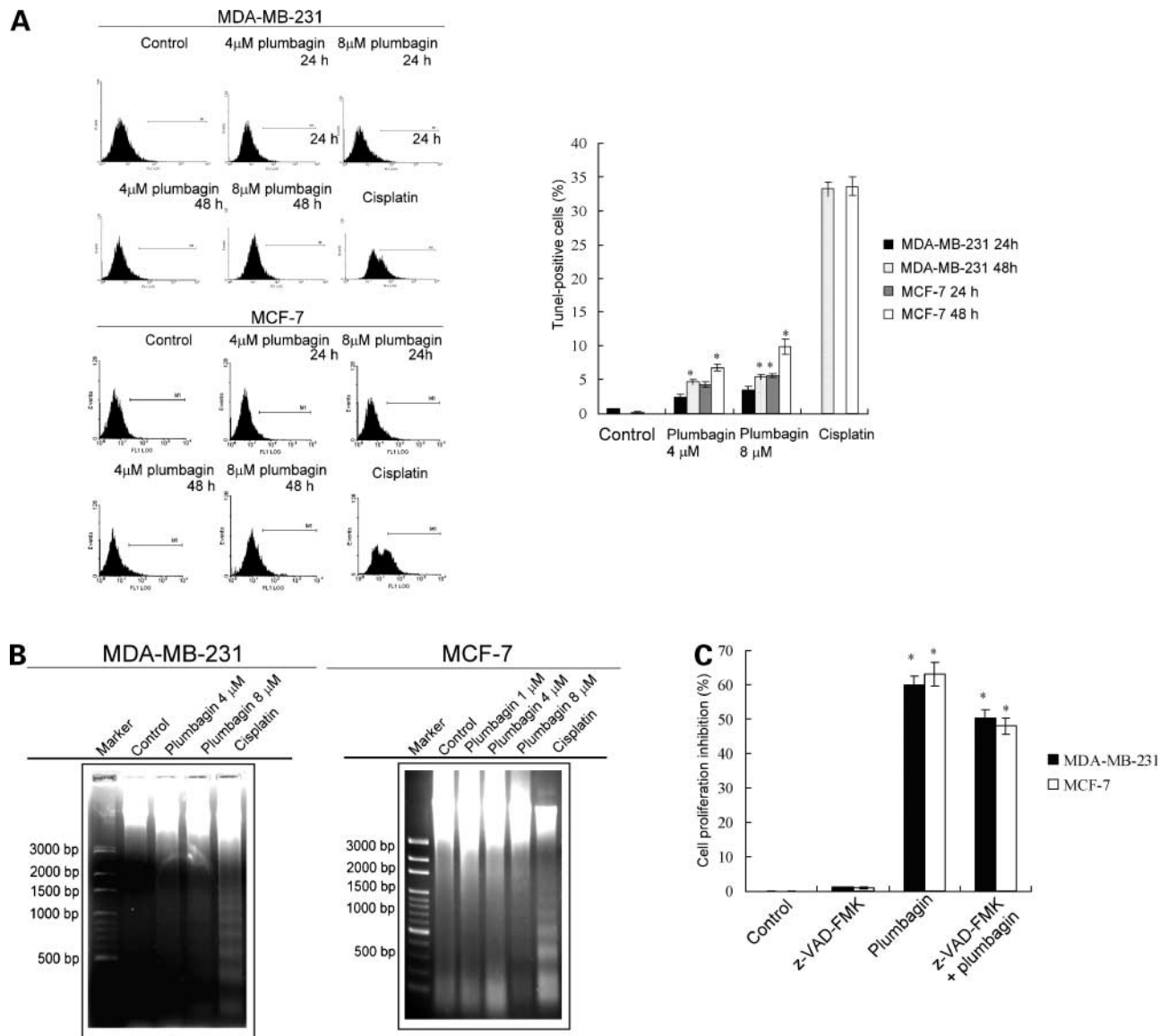


**Figure 3.** The effect of plumbagin on apoptosis induction in breast cancer cells. Plumbagin induces only small amount of apoptosis in both cells lines, as determined by TUNEL (A) and agarose gel electrophoresis (B). C, effect of z-VAD-FMK on plumbagin-mediated cell proliferation inhibition. For (A), cells were treated with various concentrations of plumbagin and cisplatin for the indicated times and then stained using ApoAlert DNA Fragmentation Assay Kit. The TUNEL-positive cells were examined by flow cytometry. For (B), DNA fragmentation was assessed by agarose gel electrophoresis. For (C), cells were treated with z-VAD-FMK (20 μmol/L) for 1 h and then 8 μmol/L plumbagin was added and incubated for 48 h. Cell proliferation was assessed by XTT. Representative of three independent experiments. \*,  $P < 0.05$ , control versus plumbagin-treated cells.

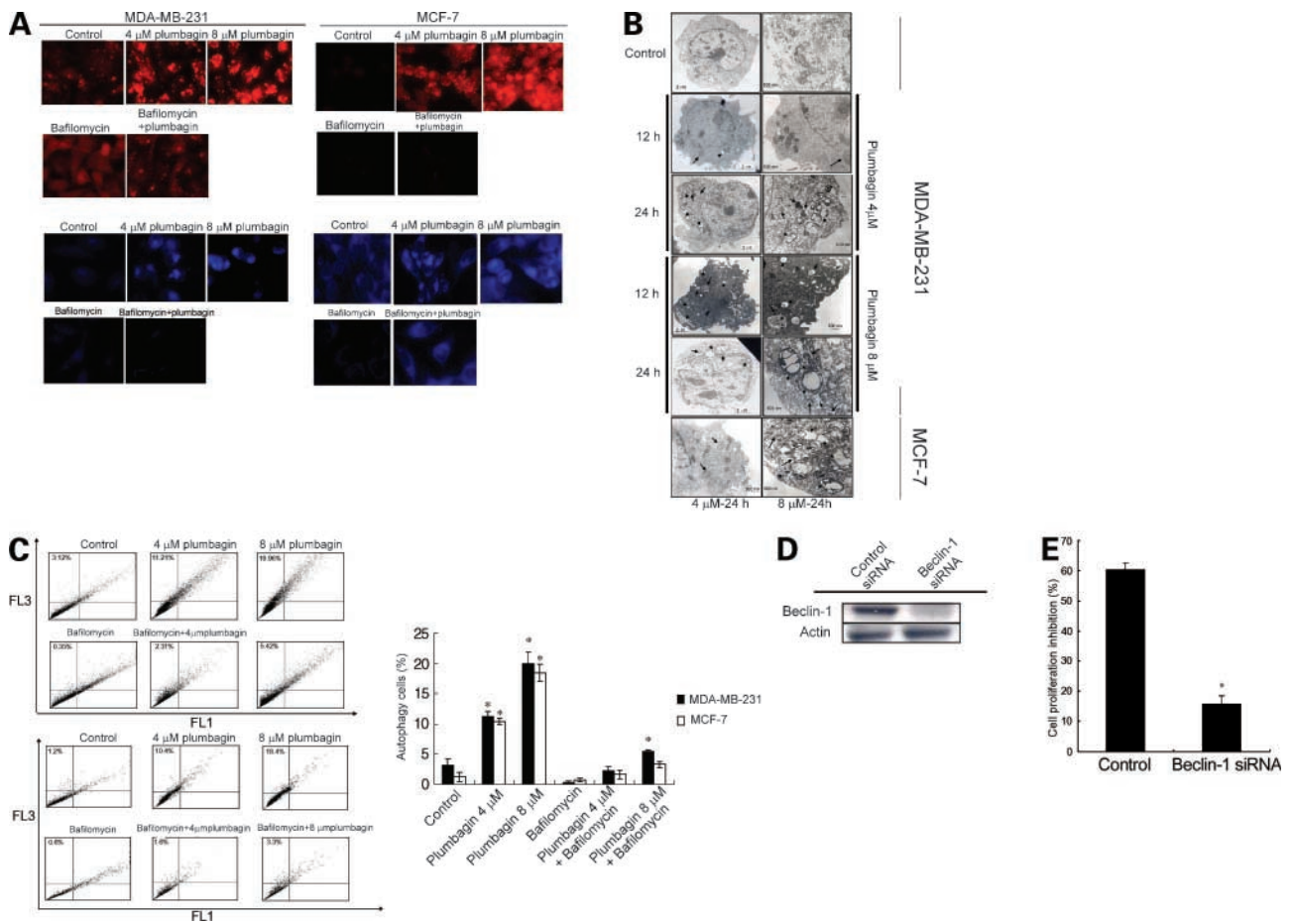


**Figure 4.** Plumbagin induces autophagic cell death in two human breast cancer cells. **A**, plumbagin-treated cells were stained with acridine orange and monodansylcadaverine (*MDC*). **B**, appearances of autophagocytic vacuoles were examined by transmission electron microscopy. Numerous autophagic vacuoles (*arrows*) and empty vacuoles (*arrowheads*) were observed. **C**, quantification of acridine orange staining using flow cytometry. **D**, inhibition of Beclin-1 expression by siRNA transfection. **E**, effect of reducing Beclin-1 siRNA on plumbagin-mediated cell proliferation inhibition. Representative of three independent experiments. \*,  $P < 0.05$ , control versus plumbagin-treated cells.

downstream target of PI3K/AKT, which may inhibit cell growth and induce autophagy. Similar responses were observed for the phosphorylated forms of two other AKT downstream targets, GSK-3 $\beta$  (Ser<sup>9</sup>) and FKHR (Ser<sup>256</sup>). To determine the change of mTOR in plumbagin-treated MDA-MB-231 and MCF-7 cells, we also examined the phosphorylation of two downstream effectors of mTOR signaling, p70S6K and 4E-BP1. The results showed that phosphorylation levels of both p70S6K (phospho-p70S6K) and 4E-BP-1 (phospho-4E-BP1) decreased, revealing a potent inhibitory effect of plumbagin on AKT/mTOR signaling.

Plumbagin-mediated inhibition of AKT was additionally confirmed by determining phosphorylation of one of its substrates, GSK-3 $\alpha/\beta$ . As shown in Fig. 5B, in comparison with the control, the Ser<sup>21</sup>/Ser<sup>9</sup> phosphorylation of GSK-3 $\alpha/\beta$  decreased after MDA-MB-231 and MCF-7 cells were exposed for 1 h to 8  $\mu$ mol/L plumbagin. Phosphorylation of GSK-3 $\alpha/\beta$  decreased relative to the control at all four time points (Fig. 5B). These

results suggest the inhibitory potential of plumbagin against the PI3K/AKT pathway, which is highly activated during the development and progression of breast cancer.

#### The Role of AKT Pathway in Plumbagin-Mediated Autophagy

Our results show that plumbagin targets the AKT signaling pathway. We next used genetic inhibition to specifically inhibit AKT to assess the consequences of AKT inhibition on plumbagin-mediated autophagy. To do so, MDA-MB-231 cells were transfected with a pool of siRNA targeting AKT, after which the cells were exposed to 8  $\mu$ mol/L plumbagin for a specific time. As shown in Fig. 6A, AKT siRNA reduced AKT expression by ~60% in comparison with control siRNA. Reduction of AKT expression by transfection of cells with AKT siRNA had no significant effect on MDA-MB-231 autophagy, suggesting that the remaining AKT activity is high enough to maintain survival of the cells. However, treatment with plumbagin significantly increased more the number of autophagy cells

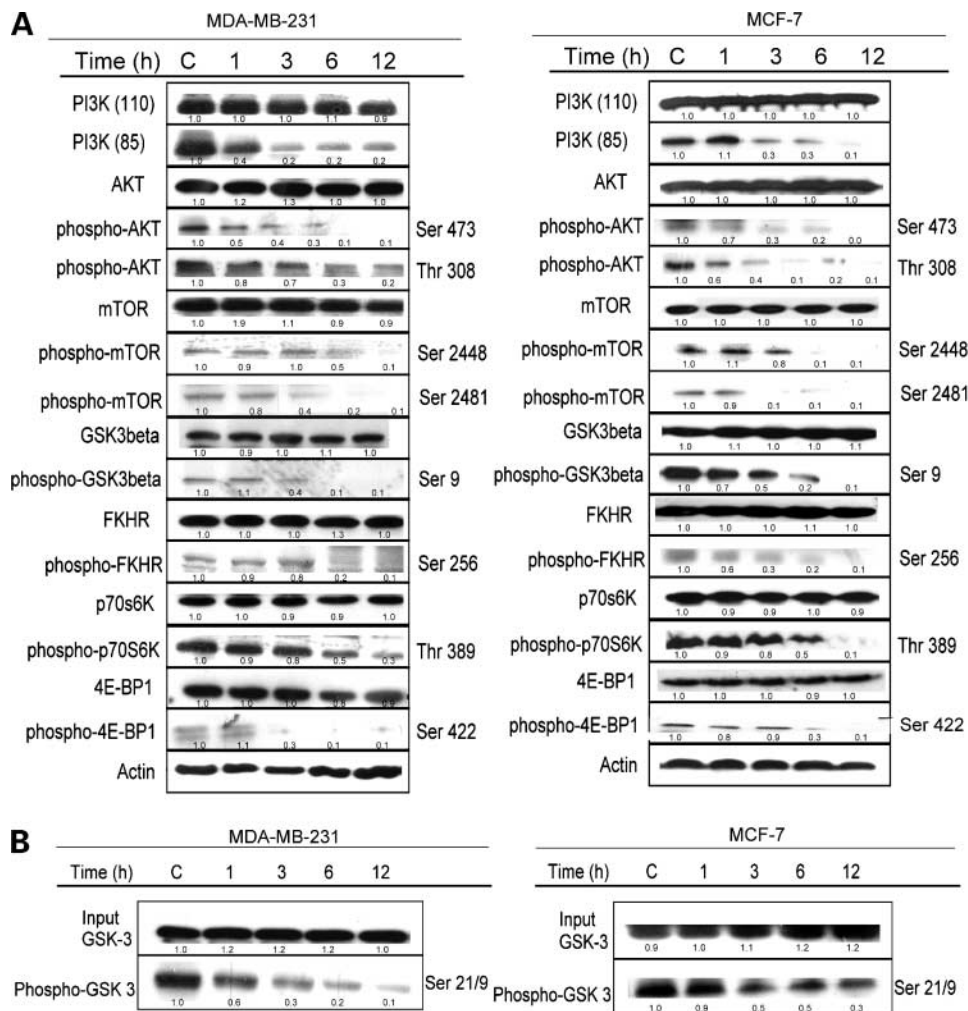


**Figure 5.** Plumbagin inhibits the expression and activity of PI3K/AKT/mTOR pathway. **A**, effect of plumbagin on the levels of PI3K, AKT, GSK, FKHR, mTOR, p70S6K, 4E-BP1, and their phosphorylated forms. **B**, effect of plumbagin on AKT activity. For **(A)**, the cells were treated with 8  $\mu$ mol/L plumbagin at different times. The control cells received an equal volume of DMSO. The cell lysates were prepared and Western blotting was done with antibodies against various PI3K/AKT/mTOR and phospho-AKT/mTOR signaling proteins. For **(B)**, the AKT kinase activity was determined using an AKT assay activity kit from Cell Signaling Technology according to the manufacturer's instructions. Representative of three independent experiments.

in AKT siRNA-transfected cells than in control siRNA-transfected cells after 24-h treatment (Fig. 6B and C). This may be due to plumbagin treatment having decreased the level of AKT activity below the threshold for maintaining normal cell survival under these conditions. Thus, this siRNA result further confirms that the AKT signaling pathway is indeed the target of plumbagin treatment.

To confirm the central role of the AKT signaling pathway as a target of plumbagin-induced autophagy, we transfected MDA-MB-231 with a constitutively active form of active AKT cDNA (Fig. 6D). AKT-overexpressing cells were treated with plumbagin and the induction of autophagy was assayed. Transfected cells expressing active AKT cDNA were considerably more resistant to plumbagin-induced autophagy than cells transfected with the

control cDNA. Plumbagin was notably unable to cause autophagy in cells transfected with active AKT cDNA, whereas plumbagin could maintain its autophagy effects on MDA-MB-231 transfected with the control cDNA (Fig. 6E and F). Therefore, it can be firmly concluded that plumbagin induces autophagic cell death in MDA-MB-231 by suppression of the AKT pathway.

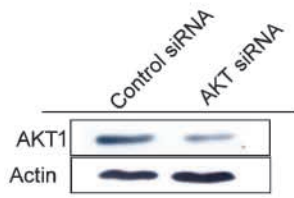
#### The Role of AKT Pathway in Plumbagin-Mediated Cell Cycle Arrest

To further evaluate the effect of AKT signaling on plumbagin-mediated G<sub>2</sub>-M arrest, AKT siRNA-transfected and AKT-overexpressing MDA-MB-231 cells were exposed to 8  $\mu$ mol/L plumbagin for a specific time, and the distributions of cell cycle and the expressions of cell cycle-related proteins were assessed. As shown in Fig. 7A,

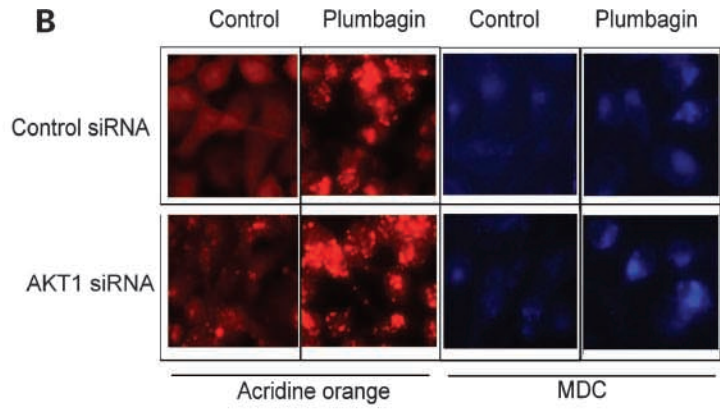
**Figure 6.** The role of AKT inhibition in plumbagin-mediated autophagic cell death. **A**, genetic suppression of AKT by AKT siRNA transfection. **B**, induction of autophagy of plumbagin in control and AKT siRNA-transfected cells. **C**, quantification of acridine orange staining using flow cytometry. **D**, overexpression of AKT by active AKT cDNA transfection. **E**, induction of autophagy by plumbagin in AKT cDNA-transfected cells. **F**, quantification of acridine orange staining by flow cytometry. MDA-MB-231 cells were transfected with control oligonucleotide, AKT siRNA, control cDNA, or active AKT cDNA, then treated with plumbagin for the indicated times. The degree of autophagic cell death was assessed by acridine orange and monodansylcadaverine staining. Representative of three independent experiments. \*,  $P < 0.05$ , control versus plumbagin-treated cells.



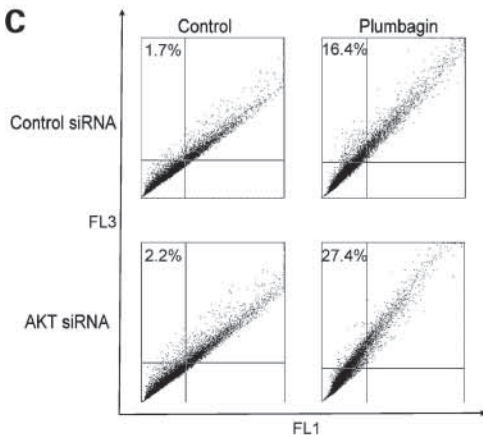
**A**



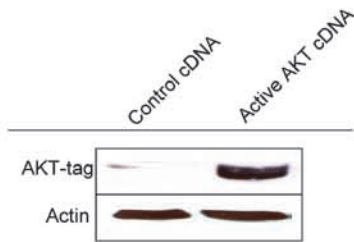
**B**



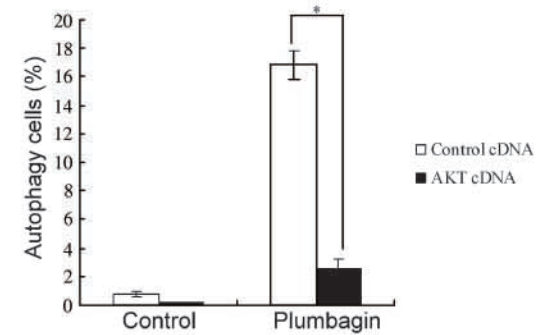
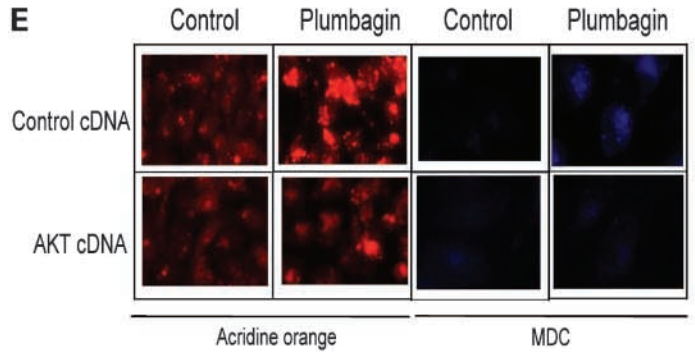
**C**



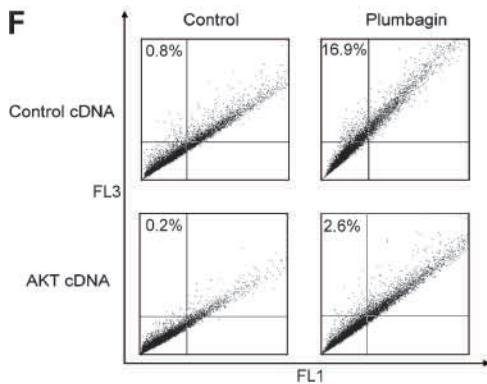
**D**



**E**



**F**



reduction of AKT expression by transfection of cells with AKT siRNA had a slight effect on the cell population at the G<sub>2</sub>-M phase. However, treatment with plumbagin significantly increased more the cell population at the G<sub>2</sub>-M phase in AKT siRNA-transfected cells than in control siRNA- and AKT siRNA-transfected cells after 6-h treatment. Decrease of AKT expression by transfection of cells with AKT siRNAs had a slight effect on phosphorylation of Cdc25C, Cdc2, and Chk2, but plumbagin greatly increased the inactive phosphorylation of Cdc25C and Cdc2 and the active phosphorylation of Chk2 when compared with cells transfected with the control and AKT siRNA (Fig. 7B).

On the other hand, transfected cells expressing active AKT cDNA were considerably more resistant to plumbagin-mediated G<sub>2</sub>-M arrest when compared with cells transfected with the control cDNA (Fig. 7C). Furthermore, plumbagin-induced inactivated phosphorylation of Cdc25C and Cdc2 and activated phosphorylation of Chk2 were significantly prevented by active AKT cDNA transfection in MDA-MB-231 cells (Fig. 7D).

#### Plumbagin Inhibits Tumor Growth in Nude Mice

To determine whether plumbagin inhibits tumor growth *in vivo*, equal numbers of MDA-MB-231 cells were injected s.c. into both flanks of nude mice. Tumor growth inhibition was most evident in mice treated with plumbagin at 2 mg/kg/d, where an ~70% reduction in tumor size was observed. In contrast with mice treated with the vehicle (Fig. 8A and B), no sign of toxicity, as judged by parallel monitoring of body weight and tissue sections of lungs, livers, and kidneys, was observed in plumbagin-treated mice (Fig. 8C). Furthermore, the transmission electron microscopy data also showed an increase of autophagocytic vacuoles in the tumors of the plumbagin-treated mice when compared with the tumors of vehicle-treated mice (Fig. 8D).

To gain insight into the mechanism of plumbagin inhibition of tumor growth *in vivo*, we harvested the MDA-MB-231 tumor xenografts from vehicle-treated and plumbagin-treated mice after treatments. We also extracted proteins to assess for levels of PI3K/AKT/mTOR proteins. As shown in Fig. 8E, decreases of PI3K (p85) regulatory subunit and phospho-AKT were observed in the tumors of the plumbagin-treated mice in comparison with the tumors of vehicle-treated mice. In addition, the levels of phospho-mTOR were lower in the tumors from the plumbagin-treated group when compared with the tumors from vehicle-treated mice.

## Discussion

Breast cancer is the most common human neoplasm in both developed and developing countries (30). In our study, we have found that plumbagin effectively inhibits tumor cell growth *in vitro*, concomitant with induction of cell cycle arrest and autophagic cell death; further, it inhibits tumor cell growth in nude mice.

In our study, we have found that plumbagin decreases the expression of cyclin B1, cyclin A, Cdc25C, and Cdc2, whereas it increases the amount of p21/WAF1 and

phosphorylation of Cdc2, phospho-Cdc25C, and phospho-Chk2. Our results show that plumbagin induces phosphorylation of Cdc25C (Ser<sup>216</sup>) through Chk2 activation and remains Cdc25C inactive. Further downstream, inactivated Cdc2 was not dephosphorylated by Cdc25C. Therefore, Cdc2 accumulated in an inactive phosphorylated state (Tyr<sup>15</sup>), resulting in cells that were unable to move through the mitotic phase. Furthermore, because the association of p21/WAF1 and Cdc2 also increased in plumbagin-treated MDA-MB-231 and MCF-7 cells, we suggest that plumbagin may prove to be a valuable tool for inhibition of Cdc2/cyclin B1 and Cdc2/cyclin A complex in breast cancers for the following reasons: (a) the down-regulation of plumbagin on cyclin B1 and cyclin A expression; (b) the induction of p21/WAF1 by plumbagin, which may subsequently inhibit the function of Cdc2 by forming Cdc2/p21/WAF complex; and (c) the increase in activated phospho-Chk2 followed by an increase in inactivated phospho-Cdc25C, suggesting that an increase in Chk2 activation is followed by an increase in Cdc25C, which loses phosphatase function for dephosphorylating and activating Cdc2.

In the present study, we showed that plumbagin induced autophagic cell death but not primarily apoptosis in MDA-MB-231 and MCF-7 cells. Some types of cancer cells exhibit autophagic changes after treatments with irradiation and chemotherapeutic drugs (4, 5, 31). Autophagy begins with the sequestering of cytosolic components, often including intracellular organelles within double-membrane structures. The vacuoles (also called autophagosomes) undergo acidification after maturation. Finally, autophagosomes fuse with lysosomes and their material is digested by lysosomal hydrolases (1, 2). Our results show that the formations of acidic vesicular organelles in MDA-MB-231 cells are characterized by acridine orange and monodansylcadaverine stain after exposures to plumbagin. Moreover, plumbagin-mediated autophagy is blocked by bafilomycin, an autophagy inhibitor. In contrast, the typical characteristic of apoptosis, DNA fragmentation, determined by DNA ladder pattern and TUNEL, is either slight or not observable in plumbagin-treated MDA-MB-231 cells. It is still unclear whether autophagy suppresses tumorigenesis or provides cancer cells with a protective response under unfavorable conditions, although several studies have reported that autophagy is triggered in cancers in response to various anticancer agents, including As<sub>2</sub>O<sub>3</sub>, tamoxifen, and temozolomide (4, 5, 32, 33). However, whether or not the initiation of different types of cell death is influenced by different stimuli, cell types, and cell content requires further investigation.

PI3K/AKT signaling is the major pathway in breast cancer cells and plays a variety of physiologic roles, including cell growth, cell cycle regulation, migration, and survival (8). Activated AKT in turn signals to a variety of key downstream molecules including mTOR, GSK-3, and FKHR, the consequence of which is to inhibit cell death and promote cell survival (8). Recent studies have indicated that inhibition of the AKT/mTOR

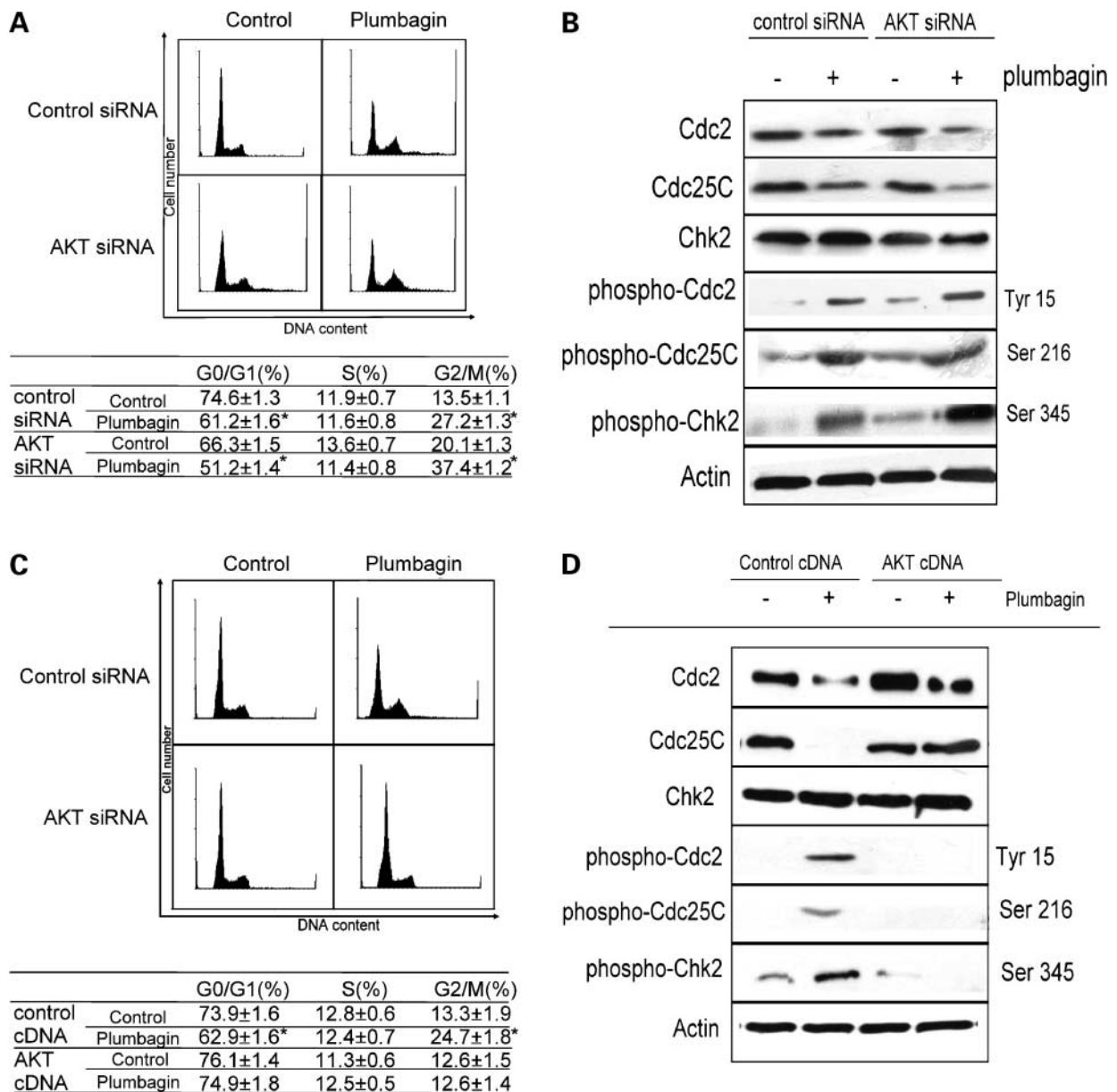


**Figure 7.** The role of AKT inhibition in plumbagin-mediated cell cycle arrest. **A**, influence of AKT inhibition by siRNA in plumbagin-mediated G<sub>2</sub>-M arrest. **B**, expression of Chk2 and phospho-Chk2 in siRNA-transfected cells treated with or without plumbagin. **C**, influence of AKT overexpression by active AKT cDNA transfection on plumbagin-mediated G<sub>2</sub>-M arrest. **D**, expression of Chk2 and phospho-Chk2 in AKT cDNA-transfected cells treated with or without plumbagin. MDA-MB-231 cells were transfected with control oligonucleotide, AKT siRNA, control cDNA, or active AKT cDNA, then treated with plumbagin for the indicated times (3 h for cell cycle-related proteins and 6 h for cell cycle analysis). The expressions of various proteins were assessed by Western blotting analysis. Cell cycle distribution was determined by flow cytometry analysis. \*,  $P < 0.05$ , control versus plumbagin-treated cells.

pathway has consistently been associated with triggering autophagy in cancer cells (2, 11–13). Our results show that plumbagin treatment decreases the expression of PI3K p85 regulatory subunit, followed by a decrease of AKT activation and activity. The inhibitory effects of plumbagin on PI3K/AKT are correlated with the loss of phosphorylation of AKT downstream targets, GSK-3 and FKHR. In addition, exposure to plumbagin also inactivated mTOR and reduced phosphorylation of its down-

stream targets (p70S6K and 4E-BP1). Moreover, enforced expression of AKT by active AKT cDNA transfection significantly diminished plumbagin-mediated autophagic cell death. In contrast, selective knockdown AKT expression by AKT siRNA-based inhibition increased plumbagin-induced autophagy. Together, these findings indicate that plumbagin induces autophagic cell death through PI3K/AKT/mTOR inhibition in human breast cancer cells.

AKT has been reported to function as a G<sub>2</sub>-M initiator (34, 35). The AKT activation inhibits initiation of the G<sub>2</sub> checkpoint in human cancer cells exposed to radiation and anticancer agents such as cytotoxic methylating agents (35). The suppression mechanism of AKT on G<sub>2</sub> arrest is not well understood, although it has been observed that AKT-mediated G<sub>2</sub> checkpoint inhibition is associated with suppression of Chk2 activation and up-regulation of cyclin B and Cdc2 expression (34, 35). Furthermore, AKT promotes cell cycle progression at the G<sub>2</sub>-M transition through Wee1Hu inactivation in mammalian cells (36). In our study, we found that inhibition of AKT was involved in the accumulation of inactive phospho-Cdc2 and phospho-Cdc25C, which may be due to the increase of Chk2 activation, leading to subsequent G<sub>2</sub> arrest. These effects, however, were abolished in MDA-MB-231 cells overexpressing AKT cDNA. The present data clearly suggest that the inhibition of AKT pathways plays a role in inducing the G<sub>2</sub> checkpoint in MDA-MB-231 cells following plumbagin exposure.

In conclusion, this study shows that (a) the breast cancer cell line MDA-MB-231 is highly sensitive to growth inhibition by plumbagin both *in vitro* and *in vivo*; (b) reduced survival of breast cancer cells after exposure to plumbagin is associated with G<sub>2</sub>-M phase cell cycle arrest and autophagic cell death; (c) plumbagin can inhibit cell cycle progression at the G<sub>2</sub>-M phase by increasing p21/Cdc2 interaction and Chk2 activation, as well as decreasing the expression of Cdc2, Cdc25C, cyclin B1, and cyclin A; and (d) plumbagin-induced autophagic cell death in the human breast cancer cells is mediated by inhibition of the PI3K/AKT/mTOR pathway. Finally, (e) it has also been shown that AKT inhibition by plumbagin may also operate in cell cycle arrest by increasing Chk2 activation. These data provide a basic mechanism for the chemotherapeutic properties of plumbagin in breast cancer cells. Future *in vivo* studies using human patients would ascertain whether this cell growth inhibition effect of plumbagin might contribute its overall chemotherapy effects in the fight against breast cancer and possibly have future therapeutic applications.

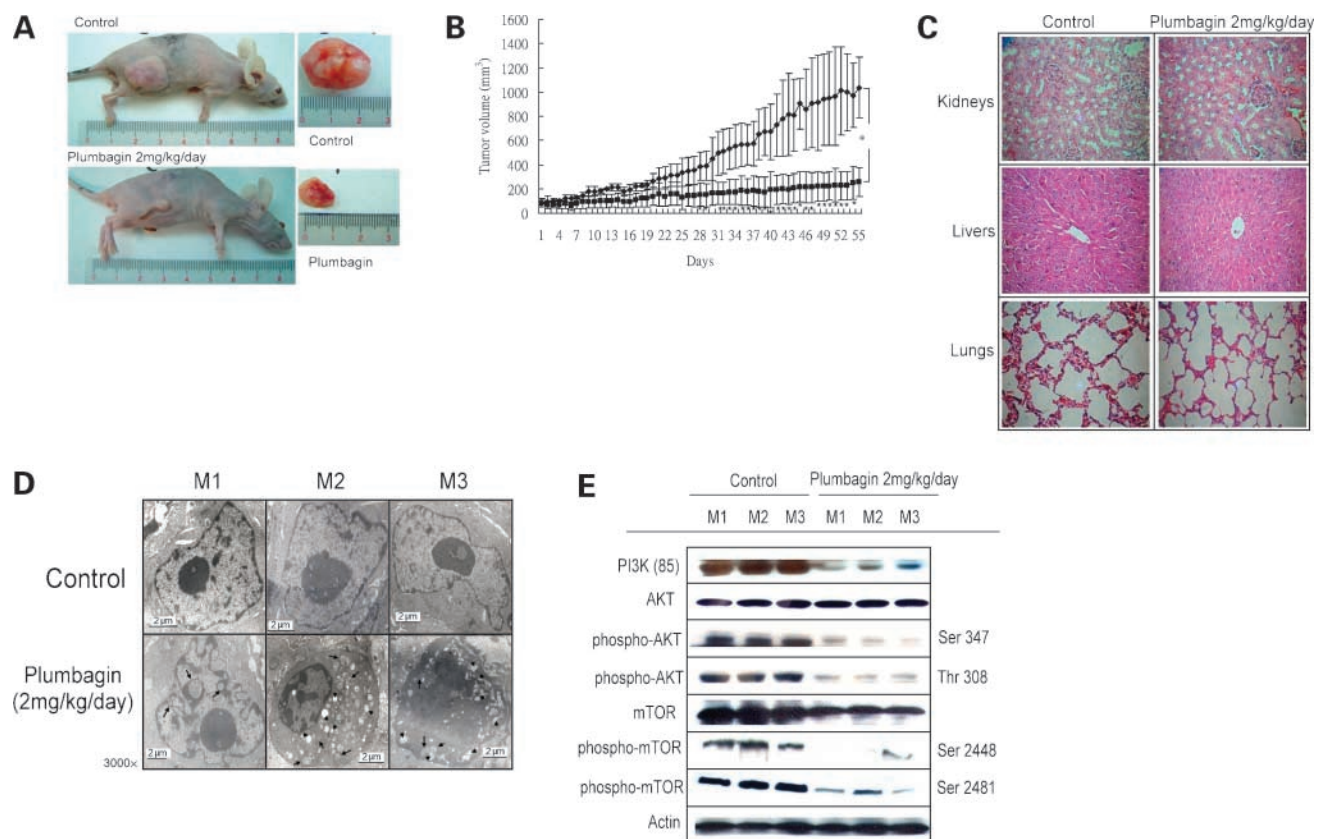


**Figure 8.** Plumbagin inhibits growth of MDA-MB-231 in nude mice. **A**, representative tumor-possessing nude mice and tumors from the control and plumbagin-treated groups. **B**, mean of tumor volume measured at the indicated number of days after implant. **C**, tissue sections of livers, lungs, and kidneys of plumbagin-treated nude mice stained with H&E. **D**, plumbagin-induced autophagic cell death in the tumors of nude mice, as determined by transmission electron microscopy. Numerous autophagic vacuoles (arrows) and empty vacuoles (arrowheads) were observed. **E**, plumbagin inhibits the expression levels of PI3K/AKT/mTOR signaling protein in MDA-MB-231 xenograft. Animals bearing preestablished tumors ( $n = 15$  per group) were dosed daily for 60 d with i.p. injections of plumbagin (2 mg/kg/d) or vehicle. During the 60-d treatment, tumor volumes were estimated by measurements taken by external calipers (mm<sup>3</sup>). The levels of various PI3K/AKT/mTOR signaling proteins were assessed by immunoblot analysis. *Columns*, mean of three determinations; *bars*, SD.

## Acknowledgments

We thank Professor Chun-Ching Lin (Graduate Institute of Natural Products, Kaohsiung Medical University, Kaohsiung, Taiwan) for providing nude mice and experiment space.

## References

- Shintani T, Klionsky DJ. Autophagy in health and disease: a double-edged sword. *Science* 2004;306:990–5.
- Kondo Y, Kanzawa T, Sawaya R, Kondo S. The role of autophagy in cancer development and response to therapy. *Nat Rev Cancer* 2005;5:726–34.
- Kroemer G, Jaattela M. Lysosomes and autophagy in cell death control. *Nat Rev Cancer* 2005;5:886–97.
- Paglin S, Hollister T, Delohery T, et al. A novel response of cancer cells to radiation involves autophagy and formation of acidic vesicles. *Cancer Res* 2001;61:439–44.
- Kanzawa T, Kondo Y, Ito H, Kondo S, Germano I. Induction of autophagic cell death in malignant glioma cells by arsenic trioxide. *Cancer Res* 2003;63:2103–8.
- Petiot A, Ogier-Denis E, Blommaert EF, Meijer AJ, Codogno P. Distinct classes of phosphatidylinositol 3'-kinases are involved in signaling pathways that control macroautophagy in HT-29 cells. *J Biol Chem* 2000;275:992–8.
- Zhao JJ, Gjoerup OV, Subramanian RR, et al. Human mammary epithelial cell transformation through the activation of phosphatidylinositol 3-kinase. *Cancer Cell* 2003;3:483–95.
- Hennessy BT, Smith DL, Ram PT, Lu Y, Mills GB. Exploiting the PI3K/AKT pathway for cancer drug discovery. *Nat Rev Drug Discov* 2005;4:988–1004.
- Kraus AC, Ferber I, Bachmann SO, et al. *In vitro* chemo- and radio-resistance in small cell lung cancer correlates with cell adhesion and constitutive activation of AKT and MAP kinase pathways. *Oncogene* 2002;21:8683–95.
- Kirkegaard T, Witton CJ, McGlynn LM, et al. AKT activation predicts outcome in breast cancer patients treated with tamoxifen. *J Pathol* 2005;207:139–46.
- Takeuchi H, Kondo Y, Fujiwara K, et al. Synergistic augmentation of rapamycin-induced autophagy in malignant glioma cells by phosphatidylinositol 3-kinase/protein kinase B inhibitors. *Cancer Res* 2005;65:3336–46.
- Guertin DA, Sabatini DM. An expanding role for mTOR in cancer. *Trends Mol Med* 2005;11:353–61.
- Paglin S, Lee NY, Nakar C, et al. Rapamycin-sensitive pathway regulates mitochondrial membrane potential, autophagy, and survival in irradiated MCF-7 cells. *Cancer Res* 2005;65:11061–70.
- Sancar A, Lindsey-Boltz LA, Unsal-Kacmaz K, Linn S. Molecular mechanisms of mammalian DNA repair and the DNA damage checkpoints. *Annu Rev Biochem* 2004;73:39–85.
- De Souza CP, Ellem KA, Gabrielli BG. Centrosomal and cytoplasmic Cdc2/cyclin B1 activation precedes nuclear mitotic events. *Exp Cell Res* 2000;257:11–21.
- Harvey SL, Charlet A, Haas W, Gygi SP, Kellogg DR. Cdk1-dependent regulation of the mitotic inhibitor Wee1. *Cell* 2005;122:407–20.
- Tyagi A, Singh RP, Agarwal C, Siriwardana S, Sclafani RA, Agarwal R. Resveratrol causes Cdc2-tyr15 phosphorylation via ATM/ATR-Chk1/2-Cdc25C pathway as a central mechanism for S phase arrest in human ovarian carcinoma Ovar-3 cells. *Carcinogenesis* 2005;26:1978–87.
- Mossa JS, El-Ferali FS, Muhammad I. Antimycobacterial constituents from *Juniperus procera*, *Ferula communis* and *Plumbago zeylanica* and their *in vitro* synergistic activity with isonicotinic acid hydrazide. *Phytother Res* 2004;18:934–7.
- Srinivas P, Gopinath G, Banerji A, Dinakar A, Srinivas G. Plumbagin induces reactive oxygen species, which mediate apoptosis in human cervical cancer cells. *Mol Carcinog* 2003;40:201–11.
- Tilak JC, Adhikari S, Devasagayam TP. Antioxidant properties of *Plumbago zeylanica*, an Indian medicinal plant and its active ingredient, plumbagin. *Redox Rep* 2004;9:219–27.
- Ding Y, Chen ZJ, Liu S, Che D, Vetter M, Chang CH. Inhibition of Nox-4 activity by plumbagin, a plant-derived bioactive naphthoquinone. *J Pharm Pharmacol* 2005;57:111–6.
- Sugie S, Okamoto K, Rahman KM, et al. Inhibitory effects of plumbagin and juglone on azoxymethane-induced intestinal carcinogenesis in rats. *Cancer Lett* 1998;127:177–83.
- Hazra B, Sarkar R, Bhattacharyya S, Ghosh PK, Chel G, Dinda B. Synthesis of plumbagin derivatives and their inhibitory activities against Ehrlich ascites carcinoma *in vivo* and *Leishmania donovani* promastigotes *in vitro*. *Phytother Res* 2002;16:133–7.
- Shao Y, Gao Z, Marks PA, Jiang X. Apoptotic and autophagic cell death induced by histone deacetylase inhibitors. *Proc Natl Acad Sci U S A* 2004;101:18030–5.
- Munafò DB, Colombo MI. A novel assay to study autophagy: regulation of autophagosome vacuole size by amino acid deprivation. *J Cell Sci* 2001;114:3619–29.
- Freedman VH, Shin SI. Cellular tumorigenicity in nude mice: correlation with cell growth in semi-solid medium. *Cell* 1974;3:355–9.
- Shin SI, Freedman VH, Risser R, Pollack R. Tumorigenicity of virus-transformed cells in nude mice is correlated specifically with anchorage independent growth *in vitro*. *Proc Natl Acad Sci U S A* 1975;72:4435–9.
- Hsu YL, Cho CY, Kuo PL, Huang YT, Lin CC. Plumbagin (5-hydroxy-2-methyl-1,4-naphthoquinone) induces apoptosis and cell cycle arrest in A549 cells through p53 accumulation via c-jun NH<sub>2</sub>-terminal kinase-mediated phosphorylation at serine 15 *in vitro* and *in vivo*. *J Pharmacol Exp Ther* 2006;318:484–94.
- Yamamoto A, Tagawa Y, Yoshimori T, Moriyama Y, Masaki R, Tashiro Y. Bafilomycin A1 prevents maturation of autophagic vacuoles by inhibiting fusion between autophagosomes and lysosomes in rat hepatoma cell line, H-4-II-E cells. *Cell Struct Funct* 1998;23:33–42.
- Paik S. Molecular profiling of breast cancer. *Curr Opin Obstet Gynecol* 2006;18:59–63.
- Ellington AA, Berhow MA, Singletary KW. Inhibition of Akt signaling and enhanced ERK1/2 activity are involved in induction of macroautophagy by triterpenoid B-group soyasaponins in colon cancer cells. *Carcinogenesis* 2006;27:298–306.
- Bilir A, Altinoz MA, Erkan M, Ozmen V, Aydinler A. Autophagy and nuclear changes in FM3A breast tumor cells after epirubicin, medroxyprogesterone and tamoxifen treatment *in vitro*. *Pathobiology* 2001;69:120–6.
- Kanzawa T, Germano IM, Komata T, Ito H, Kondo Y, Kondo S. Role of autophagy in temozolomide-induced cytotoxicity for malignant glioma cells. *Cell Death Differ* 2004;11:448–57.
- Liang J, Slingerland JM. Multiple roles of the PI3K/PKB (Akt) pathway in cell cycle progression. *Cell Cycle* 2003;2:339–45.
- Hirose Y, Katayama M, Mirzoeva OK, Berger MS, Pieper RO. Akt activation suppresses Chk2-mediated, methylating agent-induced G<sub>2</sub> arrest and protects from temozolomide-induced mitotic catastrophe and cellular senescence. *Cancer Res* 2005;65:4861–9.
- Katayama K, Fujita N, Tsuruo T. Akt/protein kinase B-dependent phosphorylation and inactivation of WEE1Hu promote cell cycle progression at G<sub>2</sub>/M transition. *Mol Cell Biol* 2005;25:5725–37.